SARS-CoV-2 SPIKE PROTEIN IN INTESTINAL CELLS OF A PATIENT WITH COVID-19 MULTISYSTEM INFLAMMATORY SYNDROME

Juan Mayordomo-Colunga, MD PhD, Ana Vivanco-Allende, MD PhD, Inés López-Alonso, PhD, Cecilia López-Martínez, Iván Fernández-Vega, MD PhD, Helena Gil-Peña, PhD, Corsino Rey, MD PhD

PII: S0022-3476(21)01155-0

DOI: https://doi.org/10.1016/j.jpeds.2021.11.058

Reference: YMPD 12700

To appear in: *The Journal of Pediatrics*

Received Date: 1 September 2021

Revised Date: 12 November 2021

Accepted Date: 19 November 2021

Please cite this article as: Mayordomo-Colunga J, Vivanco-Allende A, López-Alonso I, López-Martínez C, Fernández-Vega I, Gil-Peña H, Rey C, SARS-CoV-2 SPIKE PROTEIN IN INTESTINAL CELLS OF A PATIENT WITH COVID-19 MULTISYSTEM INFLAMMATORY SYNDROME, *The Journal of Pediatrics* (2021), doi: https://doi.org/10.1016/j.jpeds.2021.11.058.

TITLE: SARS-CoV-2 SPIKE PROTEIN IN INTESTINAL CELLS OF A PATIENT WITH COVID-19 MULTISYSTEM INFLAMMATORY SYNDROME

AUTHORS: Juan Mayordomo-Colunga[1,2,3] MD PhD, Ana Vivanco-Allende[1,2] MD PhD, Inés López-Alonso[2,3,4] PhD, Cecilia López-Martínez[2,3], Iván Fernández-Vega[5] MD PhD, Helena Gil-Peña[1,2], PhD, Corsino Rey[1,2,6,7] MD PhD.

AFFILIATIONS:

1: Department of Pediatrics. Hospital Universitario Central de Asturias, Oviedo, Spain.

2: Instituto de Investigación Sanitaria del Principado de Asturias, Oviedo, Spain.

3: Centro de Investigación Biomédica En Red (CIBER)-Enfermedades Respiratorias. Instituto de Salud Carlos III, Madrid, Spain.

4: Instituto Universitario de Oncología del Principado de Asturias. Oviedo, Spain.

5: Department of Pathology. Hospital Universitario Central de Asturias, Oviedo, Spain.

6: Department of Pediatrics. University of Oviedo, Oviedo, Spain.

7: Maternal and Child Health and Development Research Network (REDSAMID), Institute of Health Carlos III, Madrid, Spain.

Address correspondence to: Dr. Juan Mayordomo-Colunga. Sección de Cuidados Intensivos Pediátricos. Área de Gestión Clínica de Pediatría. Hospital Universitario Central de Asturias. Avda. de Roma s/n 33011, Oviedo, Asturias. Spain. E-mails: jmc@crit-lab.org; jmcolunga@hotmail.com

C.L-M. is funded by the Ministerio de Universidades, Spain (FPU18/02965). Ministerio de Universidades had no role in the design, analysis, writing or the decision to submit the present manuscript. The other authors declare no conflicts of interest.

Portions of this study were presented at the European Society of Pediatric and Neonatal Intensive Care, June 15-18, 2021, << >>.

Abbreviations:

DIC: disseminated intravascular coagulopathy

MIS-C: Multisystem inflammatory syndrome associated to COVID-19 infection

PICU: pediatric intensive care unit

Protein S: SARS-CoV-2 spike protein

RT-PCR: reverse-transcriptase polymerase chain reaction

A previously healthy 12-year-old boy had severe SARS-CoV-2 related multisystem inflammatory syndrome (MIS-C) that was rapidly fatal. Autopsy revealed the presence of a large intracardiac thrombus. SARS-CoV-2 spike protein was detected in intestinal cells, supporting the hypothesis that viral presence in the gut may be related to the immunologic response of MIS-C.

Multisystem inflammatory syndrome associated with SARS-CoV-2 infection (MIS-C) was described during the first SARS-CoV-2 pandemic wave in Europe[1]. Days or weeks after SARS-CoV-2 infection or exposure, some children (predominantly school-aged) develop this life-threatening disease[2] Patients present with fever, gastrointestinal symptoms, high inflammatory markers and cardiogenic shock[2,4,5]. Although the pathophysiology remains unclear, MIS-C encompasses cytokine-mediated hyperinflammation[3] Requirement for intensive care is reported in 50 to 80% of cases of MIS-C, and the fatality rate is reported to be 0-2%[2,5-9] In the three reported pediatric autopsies, SARS-CoV-2 was reported in several tissues and the existence of the virus in intestinal cells was shown in one child[10]. Here, we present a case of overwhelming MIS-C in a previously healthy child, providing relevant information about autopsy findings and histologic, immunohistochemical and immunofluorescent analysis for SARS-CoV-2.

CASE PRESENTATION

A 12-year-old boy with no significant past medical history presented with symptoms that began 3 days before admission consisting of malaise, fever, maculopapular rash and diffuse abdominal pain, with diarrhea. Two family members had tested positive for

SARS-CoV-2 by reverse-transcriptase polymerase chain reaction (RT-PCR) on nasopharyngeal swab 6 weeks prior. At presentation the patient tested negative RT-PCR in nasopharyngeal swab and positive for serum SARS-CoV-2 immunoglobulin G.

Abdominal ultrasound showed inflammation of the terminal ileum and peritoneal free fluid, not consistent with appendicitis; amoxicillin-clavulanate acid and intravenous fluids were begun. Microscopic urinalysis showed no leukocytes or nitrates, although a sample was sent for culture, revealing the presence of 50000 CFU/mL of *Providencia stuartii*. Blood cultures as well as subsequent tracheal aspirate cultures were negative.

A few hours after admission he developed fluid-refractory shock and was transferred to the pediatric intensive care unit (PICU). Initial tests revealed lymphopenia and increased levels of inflammatory markers (Table I; available at www.jpeds.com). Dopamine was begun, he was intubated and was subsequently treated with adrenaline and milrinone. Antibiotic coverage was changed to cefotaxime and clindamycin. MIS-C was considered a possible diagnosis and the patient was given corticosteroids (methyl-prednisolone 50 mg/12 hours, ~1.7 mg/kg/day). An echocardiogram performed after intubation showed a slight reduction of left ventricular ejection fraction (~60%), with no other obvious abnormalities. Blood tests showed progressive increase of inflammatory markers (Table I).

The following day the child developed fever up to 42.1ºC, and was not responding to intravenous immunoglobulin and a methyl-prednisolone pulse (one gram), and required addition of noradrenaline to maintain blood pressure. Low weight molecular heparin was started and antibiotic therapy was changed to vancomycin and meropenem. Serum creatinine, procalcitonin, D-dimer, lactate dehydrogenase and cardiac markers showed an abrupt elevation (Table I). The echocardiogram was repeated, demonstrating a left

ventricular ejection fraction of ~50%, without any other anomalies. Eight hours after this second echocardiogram (45 hours after PICU admission), the child developed pulseless ventricular tachycardia not responding to cardiopulmonary resuscitation.

At autopsy macroscopically, the heart was non-dilated and had a 4x1 cm thrombus in the right ventricle, encircling one papillary muscle (Figure 1, A; available at www.jpeds.com). Other macroscopic findings are shown in Figure 1 –(available at www.jpeds.com) and in Table II. Disseminated intravascular coagulopathy (DIC) was identified in most organs. Severe inflammation was found in the intestine and the heart, and hemophagocytosis was prevalent in the bone marrow (Figure 2; available at www.jpeds.com)). Complement C4d deposits were found in microvessels of the intestine, skin, liver and heart (Figure 3; available at www.jpeds.com), but not in other organs.

To perform immunofluorescence, tissue slices were deparaffinated and antigens retrieved in citrate buffer 0.1M (pH 6). Autofluorescence was diminished using sudan black saturated solution for 30 min. Slides were then washed with PBS, permeabilized with 0.1% Triton X-100 in PBS for 15 min and blocked with 1% BSA in PBS. Slides were then incubated overnight at 4°C with a rabbit monoclonal antibody against SARS-CoV-2 spike protein (Invitrogen; MA, USA) at 1:100 dilution. The next day, slides were incubated with the corresponding secondary fluorescent antibody (Donkey IgG Alexa Fluor 594-conjugated anti-rabbit; Thermo Fisher Scientific; MA, USA) at room temperature for 45 min. Slides were coverslipped with SlowFade Diamond Mountant with DAPI (Invitrogen; MA, USA) for nuclear visualization. Immunofluorescence detected the presence of protein S (spike) in the intestine (Figure 4) and in a positive control sample (Figure 5; available at www.jpeds.com). Spike protein could not be

identified in the heart, lung or the pericecal enlarged lymph node (Figure 6; available at www.jpeds.com).

DISCUSSION

The most relevant observation in our case is the presence of spike protein in intestinal cells in a child with MIS-C. In reports of autopsies in children with MIS-C , intestinal cells were studied in only one subject, revealing the presence of SARS-CoV-2 components in the intestinal epithelium[10].

Our case has unique features, mainly the overwhelming evolution in less than 48 hours, the refractory hyperpyrexia and the cardiac thrombus. The child fulfilled all the current criteria for MIS-C, but as many clinical features are common with a bacterial septic shock, broad-spectrum antibiotics were used. The formation of a large cardiac thrombus in our case is noteworthy as this has been an uncommon complication in MIS-C[12]. Arrythmia has been reported to be one of the most frequent cardiovascular complications in MIS-C[7], ventricular tachycardia has also been reported[9].

Histologic examination of most organs revealed frequent extensive thrombosis and areas of hemorrhage, findings that are not distinguishable from other causes of DIC. Duarte-Neto,et al also reported thrombi in most organs of patients with MIS-C [10]. inflammation was present mainly in the heart and the intestine, and inflammation was described in most organs in the Duarte-Neto et al case series[10]. We cannot exclude that the short course from the onset of symptoms to death of our patient could be related to limited sites of inflammation. However, as immune activation may be primarily responsible for tissue damage, there could be a discrepancy between presence of virus and tissue inflammation, as described in adults with fatal COVID-19[13].

MIS-C has some clinical similarities with Kawasaki disease, although they appear to be distinct entities[14]. Histologically, systemic vasculitis is the main feature in KD, affecting the coronary arteries in most patients. Furthermore, inflammation is present in most organs and tissues in fatal KD[15]. By contrast, in our case, inflammation was confined to the heart and the gut, and vasculitis was not found. In our case and in other reported fatal MIS-C cases, infiltration of coronary arteries was not found[10,11].

Neither diffuse alveolar damage nor hyaline membrane formation was present in our case or in the reported MIS-C cases, except for some foci of exudative diffuse alveolar damage in one child[10]. These findings are consistent with the lack of respiratory symptoms at presentation of our patient, and the relative paucity of respiratory involvement described in MIS-C[16]. The lungs in our case and in reported cases showed congestion, edema, foci of hemorrhage and thrombi[10]. Conversely, the lungs in two patients with a pulmonary form of COVID-19 exhibited pneumonia and diffuse alveolar damage[13,17].

, the heart in our patient showed myocarditis with significant lymphocyte and macrophage infiltrate. In the other reported autopsies of patients with MIS-C, significant cardiac involvement was seen, with areas of necrosis in all. In contrast, in autopsies of two patients with acute COVID-19 infection only myocardial interstitial edema was seen[10]. Gruber et al observed reduction of peripheral blood non-classical monocytes and subsets of T lymphocytes and natural killer cells, compatible with extravasation to affected tissues[3], which is in accordance with the microscopic findings in the heart of our patient.

The presence of complement C4d in several tissues, mainly the intestine, heart, liver and skin is consistent with an underlying immunologic process. Duarte-Neto also

described positive C4d immunohistochemistry in the heart [10]. The existence of hemophagocytosis in the bone marrow in our case, and in 2 of the 3 reported MIS-C cases in the spleen as well as in the liver in one, also indicates significant immune activation[10].

SARS-CoV-2 spike protein was identified in colonic cells of our patient. This finding is in accordance with a report which described that SARS-CoV-2 RNA remains in the gastrointestinal tract for weeks in children with MIS-C[18]. the severe gut inflammation in our case and in one child in Duarte-Neto's series[10] could be related to increased permeability of the gastrointestinal mucosal barrier. the breakdown of mucosal barrier function coincides with SARS-CoV-2 antigenemia, probably instigating and driving the aberrant immune activation defining MIS-C[18]. Along with persistent antigen leakage[19] from the gut, poor antigen clearance also could play a role in MIS-C pathogenesis[18]. Carter et al reported impaired antigen presentation in this condition[5]. Furthermore, the spike protein has been hypothesized to have superantigen-like properties[20].

Gastrointestinal symptoms are the most frequent manifestation of MIS-C along with fever[2,16,18]. Predominance of this clinical presentation, along with the finding of viral components in gut cells[10] may suggest that the viral antigenic source originates from the gut[18]. Similarly, it has been described that the gut serves as a nidus for SARS-CoV-2 in adults[21].

In our child SARS-CoV-2 protein S was not observed in the lung or the heart, and in the previous report SARS-CoV-2 particles were demonstrated in the heart and lungs of all 3 children and also in liver, kidneys, spleen, brain and sweat glands[10]. Our demonstration of SARS-CoV-2 spike protein in intestinal cells by immunofluorescence supports the hypothesis that the gut is important in the pathogenesis of MIS-C.

ACKNOWLEDGEMENTS: We thank the parents, who provided consent to include their child in medical literature. We also thank Dr Santiago Melón and Dr Marta Elena Argüelles for their help in interpreting viral findings.

REFERENCES

1. Royal College of Paediatrics and Child Health (RCPCH). Guidance: Paediatric multisystem inflammatory syndrome temporally associated with COVID-19 [internet]. Available from: https://www.rcpch.ac.uk/sites/default/files/2020-05/COVID-19-Paediatric-multisystem-%20inflammatory%20syndrome-20200501.pdf last accessed July 14 2021.
2. Bautista-Rodriguez C, Sanchez-de-Toledo J, Clark BC, Herberg J, Bajolle F, Randanne PC, et al. Multisystem Inflammatory Syndrome in Children: An International Survey. Pediatrics 2021;147:e2020024554.
3. Gruber CN, Patel RS, Trachtman R, Lepow L, Amanat F, Krammer F, et al. Mapping Systemic Inflammation and Antibody Responses in Multisystem Inflammatory Syndrome in Children (MIS-C). Cell 2020;183:982-95.e14.
4. Feldstein LR, Tenforde MW, Friedman KG, Newhams M, Rose EB, Dapul H, et al. Characteristics and Outcomes of US Children and Adolescents With Multisystem Inflammatory Syndrome in Children (MIS-C) Compared With Severe Acute COVID-19. JAMA 2021;325:1074-87.
5. Carter MJ, Fish M, Jennings A, Doores KJ, Wellman P, Seow J, et al. Peripheral immunophenotypes in children with multisystem inflammatory syndrome associated with SARS-CoV-2 infection. Nat Med 2020;26:1701-7.

6. Feldstein LR, Rose EB, Horwitz S, Collins JP, Newhams MM, Son MBF, et al. Multisystem Inflammatory Syndrome in U.S. Children and Adolescents. N Engl J Med 2020;383:334-46.
7. Valverde I, Singh Y, Sanchez-de-Toledo J, Theocharis P, Chikermane A, Di Filippo S, et al. Acute Cardiovascular Manifestations in 286 Children With Multisystem Inflammatory Syndrome Associated With COVID-19 Infection in Europe. Circulation 2021;143:21-32.
8. García-Salido A, de Carlos Vicente JC, Belda Hofheinz S, Balcells Ramírez J, Slöcker Barrio M, Leóz Gordillo I, et al. Severe manifestations of SARS-CoV-2 in children and adolescents: from COVID-19 pneumonia to multisystem inflammatory syndrome: a multicentre study in pediatric intensive care units in Spain. Crit Care 2020;24:666.
9. Whittaker E, Bamford A, Kenny J, Kaforou M, Jones CE, Shah P, et al. Clinical Characteristics of 58 Children With a Pediatric Inflammatory Multisystem Syndrome Temporally Associated With SARS-CoV-2. JAMA 2020;324:259-69.
10. Duarte-Neto AN, Caldini EG, Gomes-Gouvêa MS, Kanamura CT, de Almeida Monteiro RA, Ferranti JF, et al. An autopsy study of the spectrum of severe COVID-19 in children: From SARS to different phenotypes of MIS-C. EClinicalMedicine 2021;35:100850.
11. Fox SE, Lameira FS, Rinker EB, Vander Heide RS. Cardiac Endotheliitis and Multisystem Inflammatory Syndrome After COVID-19. Ann Intern Med 2020; 173:1025-7.
12. Bigdelian H, Sedighi M, Sabri MR, Dehghan B, Mahdavi C, Ahmadi A, et al. Case Report: Acute Intracardiac Thrombosis in Children With Coronavirus Disease 2019 (COVID-19). Front Pediatr 2021;9:656720.

13. Dorward DA, Russell CD, Um IH, Elshani M, Armstrong SD, Penrice-Randal R, et al. Tissue-Specific Immunopathology in Fatal COVID-19. Am J Respir Crit Care Med 2021;203:192-201.
14. Vella LA, Rowley AH. Current Insights Into the Pathophysiology of Multisystem Inflammatory Syndrome in Children. Curr Pediatr Rep 2021 (ahead of print).
15. Amano S, F Hazama, H Kubagawa, K Tasaka, H Haebara, Y Hamashima. General pathology of Kawasaki disease. On the morphological alterations corresponding to the clinical manifestations. Acta Pathol Jpn 1980;30:681-94.
16. Carter MJ, Shankar-Hari M, Tibby SM. Paediatric Inflammatory Multisystem Syndrome Temporally-Associated with SARS-CoV-2 Infection: An Overview. Intensive Care Med. 2021;47:90-3.
17. Fox SE, Akmatbekov A, Harbert JL, et al. Pulmonary and cardiac pathology in African American patients with COVID-19: an autopsy series from New Orleans. Lancet Respir Med 2020;8:681-6.
18. Yonker LM, Gilboa T, Ogata AF, Senussi Y, Lazarovits R, Boribong BP, et al. Multisystem inflammatory syndrome in children is driven by zonulin-dependent loss of gut mucosal barrier. J Clin Invest 2021;131:e149633.
19. Vella LA, Giles JR, Baxter AE, Oldridge DA, Diorio C, Kuri-Cervantes L, et al. Deep immune profiling of MIS-C demonstrates marked but transient immune activation compared to adult and pediatric COVID-19. Sci Immunol 2021; 6: eabf7570.
20. Porritt RA, Paschold L, Rivas MN, Cheng MH, Yonker LM, Chandnani H, et al. HLA class I-associated expansion of TRBV11-2 T cells in multisystem inflammatory syndrome in children. J Clin Invest 2021;131:e146614.

21. Gaebler C, Wang Z, Lorenzi JCC, Muecksch F, Finkin S, Tokuyama M, et al. Evolution of antibody immunity to SARS-CoV-2. Nature 2021;591:639-44.

FIGURE LEGENDS

Figure 1, online. Most relevant macroscopic findings. A: non dilated heart showing a 4x1 cm thrombus in the right ventricle (white arrow), encircling one papillary muscle. Coronary arteries were patent; B-C: severely congestive lungs, showing petechiae on the external surface (1C). No thrombi were found in the pulmonary artery and main branches; D: dorsum showing a rash; E: congestive liver; F: edematous cecum mucosa; G: 9 x 2.5 cm lymphadenopathy (asterisks) found next to the cecum, which on cut sections revealed extensive areas of hemorrhage; H: kidneys showed multiple clots in calices (black arrows).

Figure 2, online. Most relevant microscopic findings. Formalin-fixed, paraffin-embedded tissue blocks were processed and hematoxylin and eosin–stained after a standardized process in the hospital pathology laboratory. A: organized cardiac thrombus, adhered to the ventricular wall (arrow); B: intense pulmonary hemorrhage; C: thrombi in pulmonary microvasculature (arrows); D: perivascular inflammatory cells (arrow) in the skin (rash area on the dorsum); E: centrilobular necrosis in the liver (30-40% of the liver exhibited this pattern); F: pericecal adenopathy showing intense necrosis secondary to thrombi (arrows); G: transmural chronic inflammation in the cecum; H: thrombi in glomerular microcirculation, square shows a glomerulus in detail, with microthrombi (arrows); I: hemophagocytosis (arrows) in bone marrow aspirate.

Figure 3, online. Immunohistochemistry of several organs. A-B: Infiltration of the heart with CD3-positive T lymphocytes (A) and CD68-positive macrophages (B); C: complement C4d deposits in heart arterioles; D-E: complement C4d deposits in the

liver, mainly in zone 3 of the lobule; F: complement C4d deposits in cecum subserous fat tissue arterioles.

Figure 4. Immunofluorescence of cecum cells of the child. The first column shows cells nuclei using DAPI staining. In the second and third columns SARS-CoV-2 S (spike) protein can be seen in red color, showing a perinuclear pattern. Images taken using confocal microscopy (Leica SP8) at 400x and 630x and processed using ImageJ (NIH).

Figure 5, online. Immunofluorescence of pharyngeal cells inoculated with SARS-CoV-2. Images were taken using confocal microscopy (Leica SP8) at 400x and 630x and processed using ImageJ (NIH). The first photography shows cells nuclei using DAPI staining. In the second and third pictures SARS-CoV-2 S (spike) protein can be seen in red color, showing a perinuclear pattern. The same protocol explained in Figure 3 was used to perform immunofluorescence. In this case, pharyngeal cells inoculated with SARS-CoV-2 were smeared and fixed with acetone.

Figure 6, online. Immunofluorescence of other organs of the child. The first column shows cells nuclei using DAPI staining. SARS-CoV-2 S (spike) protein was not observed, as shown on the second and third columns. Images were taken using confocal microscopy (Leica SP8) at 400x and 630x and processed using ImageJ (NIH). The same protocol explained in Figure 3 was used to perform immunofluorescence.

Table 2. Main macroscopic and Histopathological findings of systems/organs observed.

MACROSCOPIC FINDINGS	MICROSCOPIC FINDINGS	
Respiratory system: Lung		
Severely congestive lungs, showing petechiae on the external surface. No thrombi were found in the pulmonary artery and main branches.	Alveoli	Enlarged pneumocytes with large nuclei, type II pneumocyte hyperplasia, focal sloughing, intra-alveolar haemorrhage. No evidence of intra-alveolar neutrophil infiltration, amphophilic granular cytoplasm or viral cytopathic-like changes. No hyaline membranes were identified.
	Vessels	Oedematous and congested vessels and hyaline thrombi in microvessels. No deposits of complement C4d in the microvasculature were noted.
	Cellular components	No presence of syncytial giant cells or infiltration of immune and inflammatory (lymphocytes and monocytes). Mild increased stromal cells.
Urinary system: Kidney		
Visible clots in calices. No signs conistent with pyelonephritis	Glomerulus	Ischaemic changes, podocyte vacuolation and accumulation of plasma in Bowman's space.
	Renal tubules	Non-isometric vacuolar degeneration and oedematous epithelial cells. Focal interstitial haemorrhage.
	Vessels	Erythrocyte aggregates obstructing the lumen of capillaries without platelet or fibrinoid material, fibrin thrombus and shrinkage of capillary loops in glomeruli.
Gastrointestinal system		
Edematous cecum mucosa. A 9 x 2.5 cm lymphadenopathy was found next to the cecum, which on cut sections revealed extensive areas of hemorrhage.	Colon	Numerous infiltrating plasma cells and lymphocytes with interstitial oedema in the lamina propria. Intense oedema of submucosa with mild infiltration of immune cells. Significant deposits of complement C4d in the microvasculature. Arteriolar microthrombi.
Severely congestive liver.	Liver	Focal macrovesicular steatosis, nuclear glycogen accumulation in hepatocytes, moderate zone 3 sinusoidal dilatation with extensive centrilobular necrosis (submassive hepatic necrosis).
No other macroscopic significant findings in other parts of the gastrointestinal system.	Oesophagus	No significant changes.
	Stomach	Partial epithelial degeneration, necrosis and shedding of the gastric mucosa. Dilatation and congestion of small blood vessels. Moderate oedema of submucosa with mild infiltration of immune cells (as lymphocytes, monocytes and plasma cells).
	Pancreas	Not significant changes.
Cardiovascular system		
Non dilated heart showing a 4x1 cm thrombus in the right ventricle, encircling one papillary muscle. Coronary arteries were patent.	Heart	Significant interstitial oedema and presence of inflammatory cells. Foci of lymphocytic inflammation CD3+. Presence of diffuse mobilization and infiltration by CD68+ macrophages in the myocardium. Significant deposits of complement C4d in the microvasculature. Coronary arteries showed no signs of vasculitis, microscopy was normal.
Reproductive system		
No significant changes.		
Nervous system		

No significant changes.	
Skin	
Macular rash mainly in the dorsum, with occasional petechiae.	Vessels: Perivascular inflammatory cells, intraluminal thrombi. Significant deposits of complement C4d in the microvasculature. Epidermis: no significant alterations
Bone marrow	
	Intense hemophagocytosis
Skeletal muscle	
	Focal myonecrosis

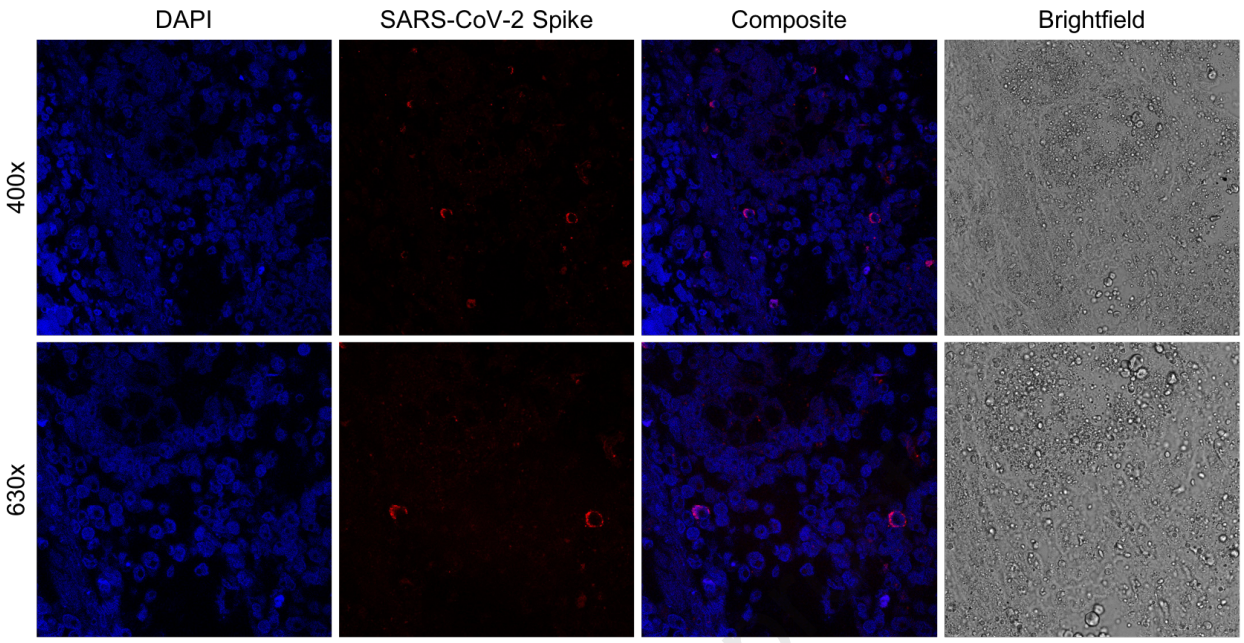

Table 1, online. Hematological and biochemical markers obtained during admission.

PICU: pediatric intensive car e unit; IL-6: interleukin 6; AST: aspartate aminotransferase; ALT: alanine aminotransferase; LDH: Lactate dehydrogenase.

	Hospital admission (-15 hours)	PICU admission (0 hours)	+10 hours	+18 hours	+28 hours	+40 hours
Hematological parameters						
Hemoglobin (g/dl)	12.2	11.1	11.4	10.3	10	-
Platelets, 10^3/µL	133	131	233	242	143	-
Leukocytes /µL	8540	10360	31110	17110	4290	-
Neutrophils/µL	7450	9420	28700	15500	3700	-
Lymphocytes/µL	510	440	1010	1110	470	-
D-dimer (ng/ml)	-	2818	3045	2538	11358	18219
Fibrinogen (mg/dl)	1224	799	840	779	532	340
Biochemical parameters						
C reactive protein (mg/dl)	28.7	31.6	33.4	27.7	22.4	16.8
Procalcitonin (ng/ml)	6.75	6.18	23.1	83.8	225	>800
IL-6 (pg/ml)	515	459	486	121	-	43
Ferritin (ng/ml)	-	871	-	-	-	-
N-terminal pro B-type natriuretic peptide (pg/ml)	-	14398	31788	35965		>70000
Cardiac Troponin T (ng/l)	-	161	360	370	495	1059
Sodium (mmol/l)	134	136	139	142	142	143
Potasium (mmol/l)	3.9	-	3.2	2.8	3.1	4.9
Urea (mg/dl)	23	42	46	49	71	102
Creatinin (mg/dl)	0.57	0.7	1.08	1.01	1.76	3.25
Albumin (g/l)	-	30	31	31	26	24

AST (U/l)	124	87	64	143	1908	5220
ALT (U/l)	138	104	92	107	844	1913
LDH (U/l)	372	-	-	549	3980	6180
Lactate (mmol/l)	-	2.7	9.3	2.4	2.8	3.5